



A correspondence principle for fractal and classical cracks

Michael P. Wnuk ^a, Arash Yavari ^{b,*}

^a College of Engineering and Applied Science, University of Wisconsin—Milwaukee, WI 53201, USA

^b School of Civil and Environmental Engineering, Georgia Institute of Technology, Atlanta, GA 30332, USA

Received 10 January 2005; received in revised form 27 June 2005; accepted 4 July 2005

Available online 2 September 2005

Abstract

In this paper we introduce a correspondence principle between fractal cracks and notches. This correspondence principle defines an equivalent smooth blunt crack for a fractal crack. Once this transformation is accomplished, the laws of linear elastic fracture mechanics apply. Since the root radius of the equivalent crack is finite, the crack may be further reduced to a notch visualized as an elongated elliptical void. Therefore, the laws of the LEFM and those of Neuber's 'notch mechanics' coincide, and they can be used interchangeably. In other words, we have shown that the three mathematical representations of discontinuities in the displacement field, a notch, a classic Griffith crack and a fractal crack, are related, and the pertinent relationships are determined by the proposed correspondence principle. We also give an estimation of the size of the plastic region ahead of a self-similar (or self-affine) fractal crack tip.

© 2005 Elsevier Ltd. All rights reserved.

Keywords: Fractal fracture; Fractal crack; Notch mechanics

1. Introduction

In fracture mechanics a crack is assumed to be a smooth surface free of stress with discontinuity in displacement field. In most materials this is a highly idealized picture for a crack. For a single crack in reality the crack surfaces are highly irregular. In some cases a crack is an idealization of a concentrated distribution of material damage. In such cases a blunt crack would be a more realistic model. One artifact of assuming a sharp crack is the singularity in the stress field at the crack tip. Even with this unrealistic characteristic the sharp crack stress solutions are useful if there is a very small plastic region around the crack tip embedded in the elastic stress field (small-scale yielding). Assuming that cracks are sharp makes fracture

* Corresponding author. Tel.: +1 626 345 2178; fax: +1 626 449 2677.
E-mail address: arash.yavari@ce.gatech.edu (A. Yavari).

mechanics problems mathematically tractable and this is the main reason for this assumption in most of the literature of fracture mechanics.

There have been extensive experimental studies on the possibility of modelling cracks by fractals. It has been experimentally established that for many materials crack surfaces are fractals in a finite range of scales. This means that one could use a fractal as a model for cracks. There are mechanical consequences if a crack is a fractal of dimension D (or roughness H in the case of self-affine cracks) [25,26]. The dependence of the order of stress singularity at the tip of a fractal crack on its fractal dimension was first realized by Mosolov [17] for self-similar fractal cracks. Using a different approach, Goldshtein and Mosolov [11,12] obtained the same expression for the order of singularity, e.g., $\alpha = \frac{D-2}{2}$. Balankin [1] studied the same problem for self-affine fractal cracks. Other interesting theoretical studies can be seen in the works of Borodich [2,3], Cherepanov et al. [6], Xie [23], Xie and Sanderson [24], and references therein. Many researchers have tried to relate the fractal dimension of a crack to its mechanical characteristics, e.g., material toughness. Universal relations do not seem to exist, though there are still some debates on this in the literature (see [4] and references therein). It is worth mentioning that in fractal fracture mechanics almost all the conclusions are at most qualitative as the boundary value problem of a fractal crack is not even well-posed.

One way of using the fractal properties of a crack may be to define an equivalent smooth defect and then carry out the analysis for the equivalent smooth defect. One choice for such a smooth defect would be a (smooth) blunt crack. In this paper we present a correspondence principle that defines an equivalent blunt crack for a given self-similar or self-affine crack. All the information about the irregularity of fracture surfaces goes into the radius of curvature of the blunt crack tip.

Significant variations from the classic solutions for crack generated stress and strain fields are demonstrated as the singularity exponent α entering in the near-tip stress field, $r^{-\alpha}$, sweeps the range $[0, \frac{1}{2}]$. This exponent is related to the fractal dimension of a crack D (or roughness H)¹ by a simple formula $\alpha = \frac{2-D}{2}$ for self-similar cracks and $\alpha = \frac{2H-1}{2H}$ for self-affine cracks. In this paper, a mathematical analysis is presented, which aims at establishing a finite crack root radius derived from a fractal crack model using some results from Wnuk and Yavari [22], see Fig. 1. This radius ρ_α turns out to depend on the (nominal) crack length and the fractal singularity exponent α . Thus, the two limiting values of ρ_α are predicted correctly, namely $\frac{a}{\pi}$ for $\alpha \rightarrow 0$ ($D \rightarrow 2$ or $H \rightarrow \frac{1}{2}$) and zero for $\alpha = \frac{1}{2}$ ($D = 1$ or $H = 1$), which describes the classic limit of a smooth sharp crack. For any known ρ_α a fractal crack can be replaced by an equivalent smooth crack with a blunt tip. This leads to a finite stress at the leading edge of the equivalent crack, σ_{\max} . The maximum stress evaluated at the edge of the blunt crack turns out to be exactly equal to the values obtained by use of the Inglis formula

$$\sigma_{\max} = \sigma \left(1 + 2 \frac{a}{b} \right) \simeq 2\sigma \sqrt{\frac{a}{\rho}} \quad \rho \ll a, \quad (1.1)$$

in which for ρ one substitutes the value predicted by our model ρ_α . Here, a and b designate the semi-axes of an elongated elliptical void, and σ denotes the far-field applied stress. This match brings the present considerations back to the starting point in the classic analysis of Griffith.

The essential results can be stated in form of a ‘correspondence principle’, as follows: For any given fractal dimension D (or roughness H) a fractal crack may be reduced to an equivalent smooth crack equipped with a finite root radius dependent on D (or roughness H). Once this transformation is accomplished, the laws of linear elastic fracture mechanics apply. Since the root radius of the equivalent crack is finite, the crack may be further reduced to a notch visualized as an elongated elliptical void. Therefore, the laws of the LEFM and those of Neuber’s [18] ‘notch mechanics’ coincide, and they can be used interchangeably.

¹ It should be mentioned that here $D(H)$ is the local fractal dimension (roughness exponent) at the crack tip. See Appendix A for more details.

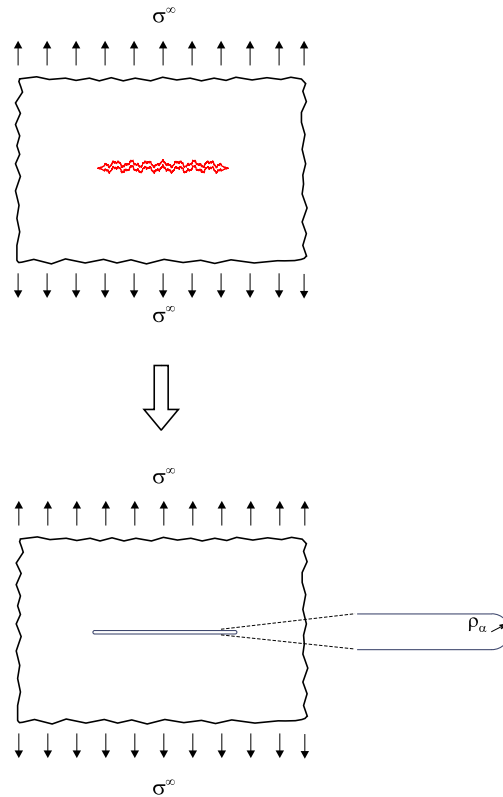


Fig. 1. A fractal crack and its equivalent smooth blunt crack.

In other words, we have shown that the three mathematical representations of the discontinuities in the displacement field, a notch, a classic Griffith crack and a fractal crack, are related, and the pertinent relationships are determined by the proposed correspondence principle.

2. Stresses generated around classic and fractal cracks. A comparison

In what follows we shall focus our attention on the equations describing the opening stress in front of a fractal crack of dimension D (or roughness H) and ahead of the smooth (but blunt) classical crack. For a fractal crack endowed with dimension D (or roughness H), or the singularity exponent $\alpha = \frac{2-D}{2}$ ($\alpha = \frac{2H-1}{2H}$), the opening stress for Mode I fracture can be evaluated using the Wnuk and Yavari's [22] Eq. (A.6) as

$$\sigma_{yy}^f(r, \theta; \alpha) = \frac{K_1^f}{(2\pi r)^\alpha} \{ \cos(\alpha\theta) + \alpha \sin \theta \sin[(\alpha + 1)\theta] \}. \quad (2.1)$$

Within the crack plane $\theta = 0$, the opening stress reads

$$\sigma_{yy}^f(r, 0; \alpha) = \frac{K_1^f}{(2\pi r)^\alpha}. \quad (2.2)$$

Here, the stress intensity factor K_1^f generalized for the case of a fractal crack is a function of the applied stress σ , the nominal crack length a , and the singularity exponent, namely

$$K_I^f = \frac{\sigma a^{\alpha-1}}{\pi^{2\alpha-\frac{1}{2}}} \int_0^a \frac{(a-x)^{2\alpha} + (a+x)^{2\alpha}}{(a^2-x^2)^\alpha} dx. \quad (2.3)$$

An alternative form of this expression reads [26]

$$K_I^f = \chi(\alpha) \sigma \sqrt{\pi a^{2\alpha}}. \quad (2.4)$$

Here, a non-dimensional function incorporates the integral in (2.4) with a non-dimensional variable $s = \frac{x}{a}$ replacing the dimensional coordinate yielding

$$\chi(\alpha) = \frac{1}{\pi^{2\alpha}} \int_0^1 \frac{(1-s)^{2\alpha} + (1+s)^{2\alpha}}{(1-s^2)^\alpha} ds. \quad (2.5)$$

This is a function continuously varying with α (D or H) from $\chi = 1$ at $\alpha = \frac{1}{2}$ to $\chi = 2$ at $\alpha = 0$, leading to the following limiting values of the K -factor

$$K_I^f = \begin{cases} \sigma \sqrt{\pi a} & \text{for } \alpha = \frac{1}{2}, \\ 2\sqrt{\pi} \sigma & \text{for } \alpha = 0. \end{cases} \quad (2.6)$$

The result for the smooth crack limit ($\alpha = \frac{1}{2}$) coincides with the LEFM value of K_I . The other limit, though, is dimensionally different from the classic solution. As can be seen K_I^f at $\alpha = 0$ ($D = 2$ or $H = \frac{1}{2}$) acquires the physical meaning of Neuber's [18] stress magnification factor valid for a stress concentrator equivalent to a void equipped with a finite root radius. For such a void the stress magnification factor, $C = 2\sqrt{\frac{a}{\rho}}$, cf. Griffith [13], enters into the equation predicting the maximum stress at the void edge, namely

$$\sigma_{\max} = 2\sqrt{\frac{a}{\rho}} \sigma. \quad (2.7)$$

From (2.6) we have $C = 2\sqrt{\pi} \simeq 3.54$, which may be compared with the value of $C = 3$ expected for a spherical void. Obviously, the discrepancy shown by these two numbers can be tolerated in the context of our simplified model of the fractal crack, which becomes less accurate when D approaches 2 (or $H \rightarrow \frac{1}{2}$) when the fractal crack degenerates to a plane-filling curve.

The problem consists in determination of the root radius of the hypothetical void visualized as an elongated ellipse or a blunt crack. In order to accomplish this task we shall employ the stress field around a blunt crack, known in the linear elastic fracture mechanics. According to Creager and Paris [7], the opening stress ahead of such a crack is asymptotically (as $r \rightarrow 0$) given as

$$\sigma_{yy} = \frac{K_I}{\sqrt{2\pi r}} \frac{\rho}{2r} \cos\left(\frac{3\theta}{2}\right) + \frac{K_I}{\sqrt{2\pi r}} \cos\left(\frac{\theta}{2}\right) \left[1 + \sin\frac{\theta}{2} \sin\frac{3\theta}{2}\right] + \dots, \quad (2.8)$$

where the origin is in the middle between the center of the circular notch and the tip. At $\theta = 0$ it reduces to

$$\sigma_{yy} = \frac{K_I}{\sqrt{2\pi r}} \left(1 + \frac{\rho}{2r}\right). \quad (2.9)$$

For a Mode I crack of length $2a$ in an infinite solid $K_I = \sigma\sqrt{\pi a}$, and the variable r is never less than $\frac{\rho}{2}$.

The early research of Creager and Paris [7] has been consequently expanded by a number of investigators. Kuang [15] developed two-term expressions for the near-tip expansions representing the components of the stress field for mixed Mode I/Mode II case. These expressions were then used to predict the crack trajectory. The founding confirmed the results of the earlier investigation by Francis and Ko [10]. Both stresses and strains in the vicinity of a blunt crack were investigated for a finite plate subject to tension by Cui et al. [8]. These authors compared the results of their theoretical studies, involving the complex stress function adjusted for finite dimensions by a weighted residues technique, with their measurements of strains via Moire method and electrical resistance gauges.

It is an established experimental fact that most cracks are highly irregular. Fractal and smooth cracks are both idealistic models of real cracks. A blunt crack is more realistic than a sharp crack. One may ask the following question. Suppose one knows from experiments that a crack is a fractal with fractal dimension D (or roughness exponent H) in some range of scales. Would it be possible to somehow use this information in the analysis of the irregular crack? The direct use of fractality is difficult as the elasticity problem of a fractal crack is not even well-posed [26]. We can think of fractal dimension as a microscopic information and one may be interested in using this information in the continuum treatment of the fractal crack. One way of using fractal information is to somehow find an equivalent blunt crack for a given fractal crack. At first glance, it may appear that this equivalent blunt crack cannot be well-defined and there are many choices. As we will show in the sequel, using stress as a measure of equivalence and postulating a property for the radius of curvature of the equivalent blunt crack, the correspondence is well-defined.

Let us now equate the stress at the front of the blunt crack, as given by Eq. (2.9) when r is replaced by half of the root radius, to the stress generated ahead of the fractal crack, see Eq. (2.2). It follows then

$$\frac{2K_I}{\sqrt{\pi\rho_\alpha}} = \frac{K_I^f}{(2\pi r)^\alpha} \Big|_{r=r^*}, \quad (2.10)$$

where r^* is a matching point. Now we need to make a decision on what value should be substituted for r in the right hand side of Eq. (2.10). We note that at $r = 0$ the stress associated with a fractal crack is singular with exception of the limiting case corresponding to $\alpha = 0$. To avoid the singularity we propose to adapt a certain finite distance from the crack tip. We expect the distance r^* to be a certain fraction of the root radius ρ_α . Note that we have attached an index α to the radius ρ in order to emphasize that the root radius for the equivalent blunt crack depends on the singularity exponent α . Thus,

$$r^* = \xi\rho_\alpha, \quad (2.11)$$

where ρ_α is the radius of curvature of the equivalent blunt crack and the coefficient ξ is to be determined by a parametric study, which follows. For $\alpha = \frac{1}{2}$, $\rho_\alpha = 0$ and we expect ρ_α to increase monotonically when α decreases from $\frac{1}{2}$ to 0. As we will see, this property can be used to find a physically reasonable value for ξ . We should emphasize that the following hypothesis will be used to find a physically reasonable value for the non-dimensional variable ξ .

Hypothesis. The radius of curvature of the equivalent blunt crack increases monotonically from 0 at $\alpha = \frac{1}{2}$ to a finite value at $\alpha = 0$.²

Substituting $r^* = \xi\rho_\alpha$ in Eq. (2.10) for r , we arrive at the following relation:

$$\frac{2\sigma\sqrt{\pi a}}{\sqrt{\pi\rho_\alpha}} = \frac{\chi(\alpha)\sigma\sqrt{\pi a^{2\alpha}}}{(2\pi\xi\rho_\alpha)^\alpha}. \quad (2.12)$$

This yields

$$\rho_\alpha(\alpha, \xi) = \frac{a}{\pi} \left[\frac{\chi(\alpha)}{2^{\alpha+1}\xi^\alpha} \right]^{\frac{2}{2\alpha-1}}. \quad (2.13)$$

² One can justify (or motivate) this hypothesis as follows. Fractal dimension is a measure of irregularity of a fracture surface. We know that a more irregular crack has a weaker stress singularity, i.e., $\alpha(D) = \frac{2-D}{2}$ is a monotonically decreasing function of D . The idea is to replace a fractal crack by a blunt crack with a finite radius of curvature. We expect the most irregular crack ($D = 2$) to correspond to a blunt crack with a positive radius of curvature. We know that the least irregular crack, i.e., a smooth crack corresponds to a blunt crack with radius of curvature $\rho = 0$. So, in some sense the radius of curvature should represent the stress singularity of the corresponding fractal crack (or equivalently its irregularity). Thus this new measure of irregularity should be a monotone function of D as well. Therefore, considering two fractal cracks with fractal dimensions $D_1 < D_2$ it is reasonable to assume that $\rho_{D_1} < \rho_{D_2}$.

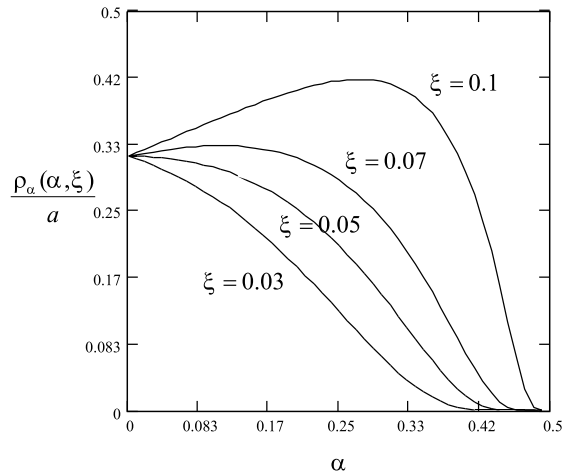


Fig. 2. Normalized radius of curvature plotted versus the fractal singularity exponent for four different values of the size parameter ξ .

The plots of the function $\rho_\alpha(\alpha, \xi)$ are shown in Fig. 2. Four curves illustrate the behavior of ρ_α for chosen values of the variable ξ , namely 0.03, 0.05, 0.07 and 0.13. Only one of these curves, depicted by the third curve from the top, satisfies the condition of zero slope at $\alpha = 0$ (for larger values of ξ there is at least one point in the curve with negative slope). This statement is reinforced by an examination of Fig. 3, in which for different values of ξ the derivative of ρ_α with respect to α is shown as a function of α . The first two curves from the top exhibit two sub-intervals, for which negative and positive values of the function occur. This is not a desirable feature, as one would expect the root radius to decrease monotonically with α , rather than increase and then decrease as indicated by the top two curves. It is seen that lowering the value for ξ reduces the derivative to negative range, as required (see the bottom curve). The transition from a two-value (negative and positive) to a single sign (negative) value for the slope occurs near the point $\xi = 0.05$. The exact value of ξ for which this transition takes place is determined by the root of the equation

$$\left. \frac{\partial \rho_\alpha(\alpha, \xi)}{\partial \alpha} \right|_{\alpha=0} = 0. \tag{2.14}$$

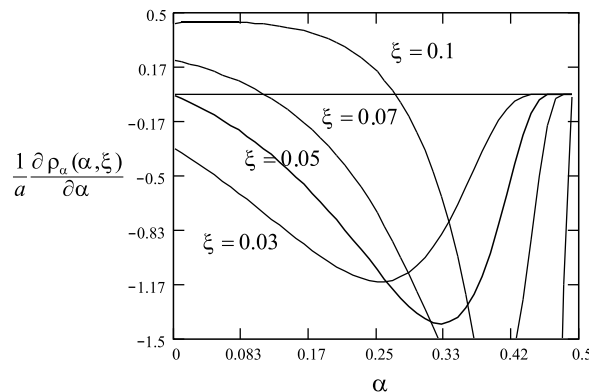


Fig. 3. Rates of change of the functions depicted in Fig. 2.

The root is $\xi_{\text{trans}} \simeq 0.05066$, and we shall round it up to 0.05. Both these numbers are somewhat below the critical value of ξ , at which the derivative of ρ_α with respect to ξ blows up at α approaching the limit $\frac{1}{2}$. The critical value of ξ can be found numerically for $\alpha \rightarrow \frac{1}{2}$ as the root of the following equation:

$$\frac{\partial \rho_{\frac{1}{2}}(\frac{1}{2}, \xi)}{\partial \xi} = 0. \quad (2.15)$$

We obtain $\xi_{\text{cr}} \simeq 0.0525$. Somewhat smaller value of ξ is determined as the transition point from double sign slope, shown in Fig. 2, to a single sign slope (see the curves drawn in Figs. 2 and 3 for $\xi = 0.05$). The obtained sequence of these specific values for ξ reads as follows: $0.05 < \xi_{\text{trans}} < \xi_{\text{cr}}$. Therefore, we conclude that if the cut-off value for ξ is established at the level of 0.05, then all the conditions posed here will be satisfied. It turns out that the physical meaning of this cut-off value is that of an upper bound for ξ . Above the value ξ_{cr} (which we shall approximate by 0.05), the rate and the function itself become unbounded, and thus they provide no physically meaningful solution for the root radius. This cut-off threshold of ξ is labeled as ϵ and referred to as the upper bound. Substituting ϵ for ξ in Eq. (2.13) yields the final form for the finite root radius of the equivalent classical crack

$$\rho_\alpha = \frac{a}{\pi} \left[\frac{2^{\alpha+1} \epsilon^\alpha}{\chi(\alpha)} \right]^{\frac{2}{1-2\alpha}}. \quad (2.16)$$

The equation predicts two limiting values of the root radius. For $D = 2$ ($H = \frac{1}{2}$ or $\alpha = 0$) we recover the limit predicted earlier, cf. Wnuk and Yavari [22], which is $\rho_\alpha = \frac{a}{\pi}$ and this corresponds to the stress magnification factor of 3.54. For the smooth crack limit, $\alpha = \frac{1}{2}$ one obtains a zero root radius, as would be expected. The root radius ρ_α is plotted as a function of the fractal dimension D and roughness H in Fig. 4. Once the radius of the crack tip is established, we can proceed to evaluate the opening stress occurring at the front of the blunt crack. Employing the formula (2.7) we have

$$\sigma_{\text{max}} = 2\sqrt{\pi}\sigma \left[\frac{\chi(\alpha)}{2^{\alpha+1} \epsilon^\alpha} \right]^{\frac{1}{1-2\alpha}}. \quad (2.17)$$

This expression yields $\sigma_{\text{max}} = 2\sqrt{\pi}\sigma$ for the limiting case of a plane filling fractal crack ($D \rightarrow 2$ or $H \rightarrow \frac{1}{2}$), while for the Griffith crack it becomes singular in agreement with Eq. (2.7). For all the intermediate values of D (or H), the maximum stress turns out to be a certain multiple of the applied stress, as depicted in Fig. 5.

3. Size of plastic zone for a fractal crack

In this section using Wnuk and Yavari's [22] estimation of fractal Mode I stress intensity factor, we generalize Irwin's [14,16] method for calculating the size of the plastic zone ahead of the crack tip for fractal cracks. Assuming that the nominal crack is along the x_1 -axis, we know that

$$\sigma_{22}(r, \theta = 0) = \frac{K_1^f}{(2\pi r)^\alpha}. \quad (3.1)$$

Stress is equal to the yield stress at the distance $r_y^f = \frac{1}{2\pi} \left(\frac{K_1^f}{\sigma_y} \right)^\frac{1}{\alpha}$ from the crack tip. The size of the plastic zone (radius of the disk) r_p^f is calculated as follows

$$\int_0^{r_y^f} \frac{K_1^f}{(2\pi r)^\alpha} dr - r_y^f \sigma_y = (r_p^f - r_y^f) \sigma_y. \quad (3.2)$$

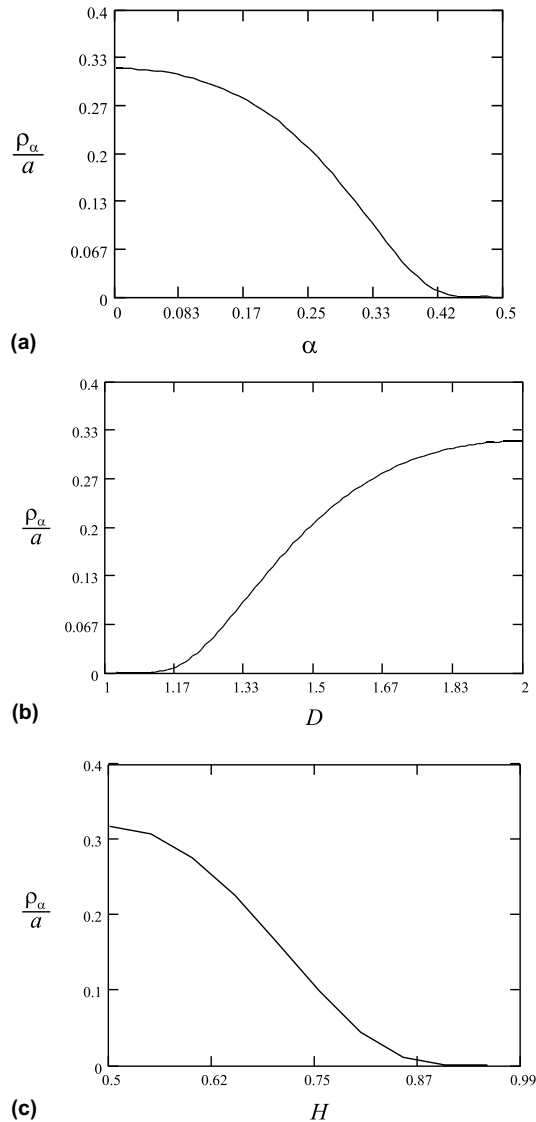


Fig. 4. (a) Variation of the fractal equivalent radius of curvature with the fractal singularity exponent α , (b) the same quantity as a function of D and (c) the same quantity as a function of H .

Thus

$$r_p^f = \frac{r_y^f}{1 - \alpha}. \tag{3.3}$$

For a Mode I fractal crack of nominal length $2a$ in an infinite solid we know that

$$K_I^f = \chi(D)\sigma\sqrt{\pi a^{2-D}}, \tag{3.4}$$

for a self-similar crack and

$$K_I^f = \psi(H)\sigma\sqrt{\pi a^{\frac{2H-1}{H}}}, \tag{3.5}$$

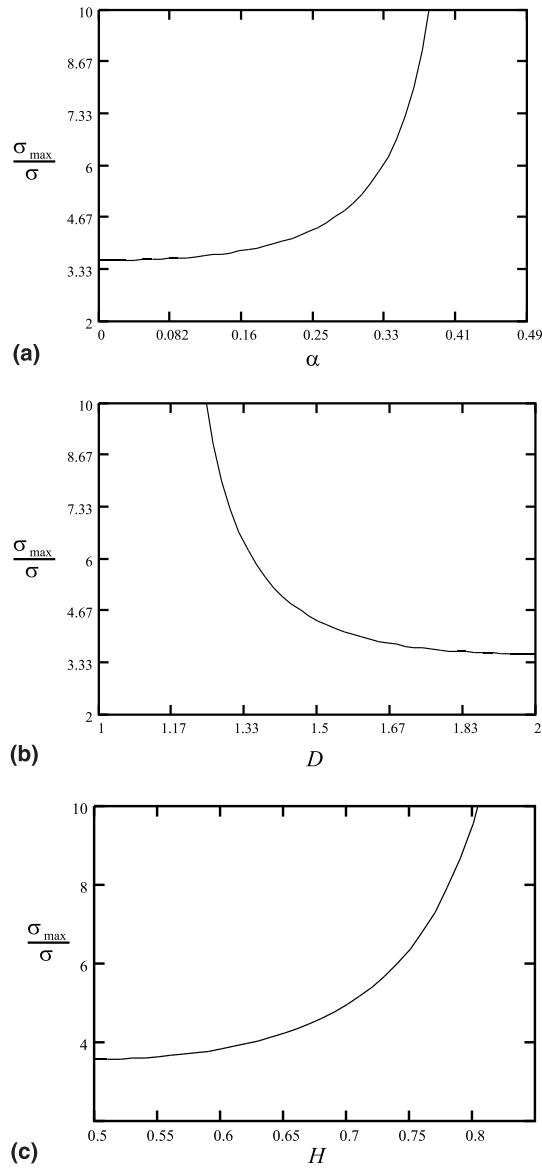


Fig. 5. (a) Maximum stress evaluated at the edge of the equivalent blunt crack as a function of the fractal singularity exponent α , (b) maximum stress as a function of D and (c) maximum stress as a function of H .

for a self-affine fractal crack, where

$$\chi(D) = \frac{1}{\pi^{2-D}} \int_0^1 \frac{(1+s)^{2-D} + (1-s)^{2-D}}{(1-s^2)^{\frac{2-D}{2}}} ds, \tag{3.6}$$

$$\psi(H) = \frac{1}{\pi^{\frac{2H-1}{H}}} \int_0^1 \frac{(1+s)^{\frac{2H-1}{H}} + (1-s)^{\frac{2H-1}{H}}}{(1-s^2)^{\frac{2H-1}{2H}}} ds. \tag{3.7}$$

Here we calculate r_p^f for both self-similar and self-affine cracks. For a self-similar crack

$$r_p^f = \frac{2}{D} \left(\frac{K_I^f}{\sigma_y} \right)^{\frac{2}{2-D}} \tag{3.8}$$

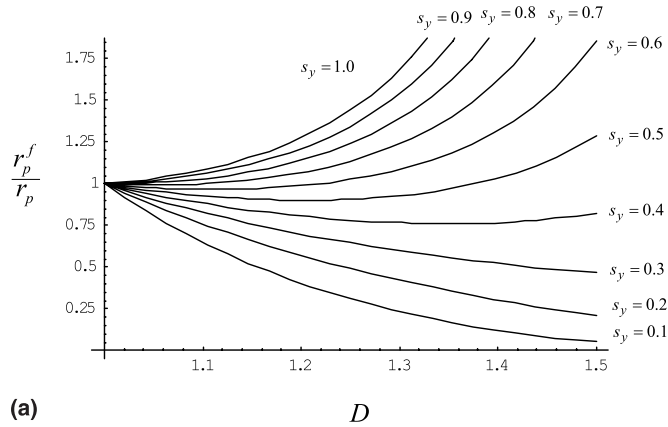
Thus

$$\frac{r_p^f}{r_p} = \frac{1}{D} \pi^{\frac{D-1}{2-D}} \chi(D)^{\frac{2}{2-D}} \left(\frac{\sigma}{\sigma_y} \right)^{\frac{2(D-1)}{2-D}} \tag{3.9}$$

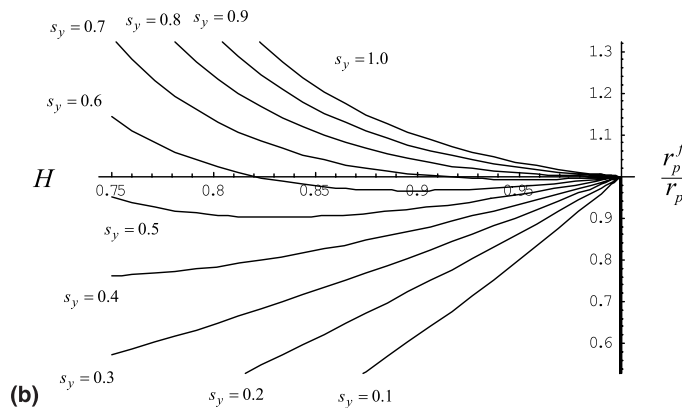
Similarly, for a self-affine crack

$$\frac{r_p^f}{r_p} = H \pi^{\frac{1-H}{2H-1}} \psi(H)^{\frac{2H}{2H-1}} \left(\frac{\sigma}{\sigma_y} \right)^{\frac{2(1-H)}{2H-1}} \tag{3.10}$$

Fig. 6 shows plots of $\frac{r_p^f}{r_p}$ as functions of D and H for different values of $s_y = \frac{\sigma}{\sigma_y}$. As Wnuk and Yavari’s [22] estimate is not accurate for very rough fractal cracks, we have plotted $\frac{r_p^f}{r_p}$ for the ranges $D \in [1, \frac{3}{2}]$ and $H \in [\frac{2}{3}, 1]$. It is seen that for a given D or H for small values of s_y ($s_y < 0.5$) the radius of the fractal plastic zone is smaller than that of the smooth crack. But for large values of s_y (given H or D) the fractal plastic



(a)



(b)

Fig. 6. (a) Size of the plastic region as a function of fractal dimension D for different values of $s_y = \frac{\sigma}{\sigma_y}$ and (b) size of the plastic region as a function of roughness exponent H for different values of $s_y = \frac{\sigma}{\sigma_y}$.

zone is larger than that of the smooth crack. For a given value of D (or H), increasing s_y increases the plastic zone size, which is not surprising.

4. Conclusions

A new concept of characteristic length parameter associated with fractal nature of fracture has been proposed. The length parameter is the finite root radius associated with an arbitrary fractal crack. Accepting a hypothesis that says ρ_α is a monotonically decreasing function in the interval $\alpha \in [0, \frac{1}{2}]$, we were able to find ρ_α as a function of α . The length parameter scales down with the singularity exponent α , see Eq. (2.16) and Fig. 4. We predicted the finite maximum stress occurring at the tip of the fractal crack for all values of the dimension D (or roughness H), excepting the limit of $D = 1$ ($H = 1$), the smooth crack limit, see Eq. (2.17) and Fig. 5.

The outcome of the application of this length parameter concept is the correspondence principle, which can be stated as follows:

Correspondence principle. For any given fractal dimension D (or roughness exponent H) a fractal crack may be reduced to an equivalent smooth crack equipped with a finite root radius dependent on D (or H).

Once this transformation is accomplished, the laws of linear elastic fracture mechanics apply. Since the root radius of the equivalent crack is finite, the crack may be further reduced to a notch visualized as an elongated elliptical void. Therefore, the laws of the LEFM and those of Neuber's 'notch mechanics' coincide, and they can be used interchangeably. The following comment is in order for justifying the Correspondence Principle.

The correspondence principle between a fractal crack and a smooth blunt crack and/or an elliptical void, as proposed in this paper, has been inspired by our earlier research, cf. Ref. [22]. There we have shown that in the limiting case when the fractal dimension D approaches 2, or when the fractal singularity exponent $\alpha \rightarrow 0$, the fractal crack behaves as an elliptical void generating a certain finite stress at the root of the crack. For $D = 2$, when fractal crack becomes a plane filling entity, this maximum stress was found to be $\sigma_{\max} = 2\sqrt{\pi}\sigma$. This result is remarkably similar to Neuber's concept of the stress magnification factor, $C = \frac{\sigma_{\max}}{\sigma}$, which for an elliptical void can be calculated from the classic equation of Inglis, $C = 1 + 2\frac{a}{b}$. For the ratio of the semi-axes $\frac{a}{b} = \sqrt{\pi} - \frac{1}{2}$, this equation yields $C = 2\sqrt{\pi}$, the same result which was obtained for a fractal crack when $D \rightarrow 2$. Another obvious analogy is the one between the limiting fractal crack case of $D = 2$ and a blunt crack. Here, all we need to know is a certain finite root radius assigned to the equivalent blunt crack. When the distribution of stress resulting from the fractal field $K_1^f(2\pi r)^\alpha$ and the one for the blunt crack $2K_1(\pi\rho)^{\frac{1}{2}}$ are set equal to each other at a certain finite distance, say $r = \rho$, then one indeed recovers a finite root radius $\rho_{D=2} = \frac{a}{\pi}$. This result is valid, though, only in the strict limit of $D = 2$ (or $\alpha = 0$), and the stress calculated at the crack root is again $2\sqrt{\pi}\sigma$. The question now arises, would such a correspondence be possible for an arbitrary fractal dimension? The answer is a qualified 'yes'. If the stresses for a fractal crack and the equivalent blunt crack are compared not at $r = 0$ (in which case the equation yields no physically meaningful result), but at $r = r^*$, where the finite distance r^* becomes now a function of the fractal dimension, which enters through the fractal singularity exponent. The symbol r^* is then changed to $\xi\rho_\alpha$ in order to emphasize the fact that this equivalent root radius depends on the fractal dimension. The function $\rho_\alpha = f(\alpha)$ is not an arbitrary function, but it is defined by the postulate of equal maximum stresses for both the fractal and the equivalent blunt crack, and it is carefully adjusted by the detailed parametric studies of the governing equation (2.13). It turns out that only a certain well defined value for r^* is admissible, and it is $r^* = \epsilon\rho_\alpha$, where ϵ was calculated in Section 2. Exact physical meaning of r^* is not well established yet, and deserves further investigation. It can, however, be connected with a certain thickness of the 'fractal boundary layer'. This connection will be a subject of a future research. The quantity ρ_α varies from $\frac{a}{\pi}$ at $\alpha = 0$ to zero at $\alpha = \frac{1}{2}$, as it would be expected for the classic sharp crack (Griffith) case. The thickness of

the fractal boundary layer, r^* , is a small fraction of ρ_α . When K_I^f is substituted into Eq. (2.2), one obtains the stress distribution

$$\frac{\sigma_{yy}}{\sigma} = \pi^{\frac{1}{2}-\alpha} \chi(\alpha) \left(\frac{2r}{a}\right)^{-\alpha} \tag{4.1}$$

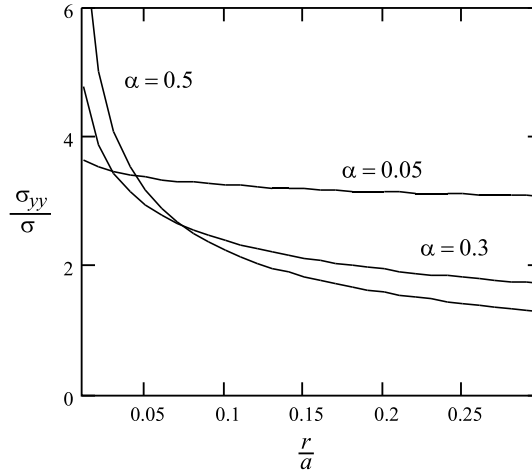


Fig. 7. Distributions of the opening stress ahead of the leading edge of a fractal crack are shown for three values of the fractal singularity exponent α . The top curve corresponds to the Griffith case yielding the singular stress at $r = 0$; while the other two cases depicted ($\alpha = 0.3$ and $\alpha = 0.05$) yield a finite stress σ_{max} at the crack tip provided that the smallest permissible distance from the tip is identified as the thickness of the ‘fractal boundary layer’. For the Griffith crack this thickness approaches zero.

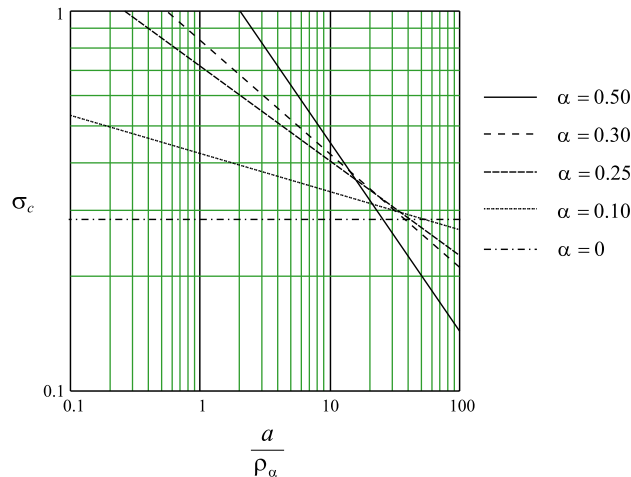


Fig. 8. Maximum stress at the tip of the fractal crack is normalized by the critical stress at fracture and plotted in the log–log scale as a function of the crack half-length normalized by the root radius, as predicted by Eq. (4.1). The parameter that distinguishes the five curves shown is the fractal exponent α varying from $\alpha = \frac{1}{2}$ to α approaching zero representing a fractal object of dimension $D = 2$. The steepest line corresponds to the LEFM result, while the horizontal line corresponds to the fractal object, for which $D = 2$ (or $\alpha = 0$). Therefore, both limiting cases of fracture representations, the LEFM and the UTS theories are recovered. These data suggest that should the fractal dimension depend on the crack length, then the results of this model would closely resemble those derived from the quantized fracture mechanics as found by Pugno and Ruoff [19] and by Taylor et al. [20], and used to describe behavior of short cracks.

This equation is valid for $r \geq \rho_\alpha$, where ρ_α is defined by (2.13). For three values of fractal dimension, as measured by the parameter α , Fig. 7 shows the resulting stress distributions ahead of a fractal crack. Note that in the interval $(0, \rho_\alpha)$ the stress is assumed constant and equal the maximum stress at the crack root. They compare very well with the available literature data, listed in Refs. [7,8,10,15] and they appear to be physically sound. Fig. 8 shows a log–log plot of maximum normalized stress at the tip of the equivalent blunt crack as a function of the normalized half crack length (a/ρ_α) . The parameter that distinguishes the five curves shown is the fractal exponent α varying from $\alpha = \frac{1}{2}$ to α approaching zero representing a fractal object of dimension $D = 2$. The steepest line corresponds to the LEFM result, while the horizontal line corresponds to the fractal object, for which $D = 2$ (or $\alpha = 0$). Therefore, both limiting cases of fracture representations, the LEFM and the UTS theories are recovered. This is in agreement with the recent results found independently—and using a different physical models, by Pugano et al. [19] and Taylor et al. [20].

Generalizing Irwin's method, we calculated the radius of plastic zone ahead of a fractal crack. Using Wnuk and Yavari's [22] estimation of K_I^f , we were able to compare the size of plastic zones of fractal and smooth cracks quantitatively.

Appendix A. Stress singularity for a scale-dependent fractal crack

Usually one property of fractals is their homogeneity, i.e., locally all the neighborhoods in a fractal set are equivalent. It is possible to have a set with variable fractal dimension. This has been observed in turbulence by Catrakis and Dimotakis [5,9] and they called such fractals 'scale-dependent fractals'. A scale-dependent fractal could be a reasonable model for a crack. Suppose one starts from a smooth crack and under applied loads the crack starts propagating quasi-statically. Assume that the crack stops at some point and that the new crack can be modelled by a curve which is smooth at the point of initial growth ($D = 1$) and becomes rougher and rougher as one approaches the new crack tip. So, suppose the crack is smooth in the interval $(-\infty, a_0)$ and is a fractal with varying fractal dimension in the interval (a_0, a) and the fractal dimension at a is D . We are interested in stress distribution very close to the crack tip. An example of a fractal curve with dimension continuously varying from 1 to 2 in the interval $[0, 1]$ is given in [21]. Now assume that stress has the following asymptotic form close to the crack tip,

$$\sigma_{ij}(r, \theta) \sim r^{-\alpha}. \quad (5.1)$$

Suppose the crack grows and the crack tip moves to the point $x = a + \Delta a$. In the growth process the fractal dimension of the new fracture surfaces may vary but we assume that fractal dimension changes continuously, say it is in the interval $(D, D + \Delta D)$. The area of the new fracture surfaces is,

$$\Delta A \sim 2(\Delta a)^D. \quad (5.2)$$

This means that,

$$\alpha = \frac{2 - D(a)}{2}, \quad (5.3)$$

i.e., the stress singularity exponent is a function of fractal dimension at the crack tip. This is not surprising as Griffith's criterion is local.

References

- [1] Balankin AS. Physics of fracture and mechanics of self-affine cracks. *Engng Fract Mech* 1997;57(2):135–203.
- [2] Borodich FM. Some fractal models of fracture. *J Mech Phys Solids* 1997;45(2):239–59.
- [3] Borodich FM. Fractals and fracture scaling in fracture mechanics. *Int J Fract* 1999;95:239–59.

- [4] Bouchaud E. Scaling properties of cracks. *J Phys: Condens Matter* 1997;9:4319–44.
- [5] Catrakis HJ, Dimotakis PE. Scale-dependent fractal geometry. In: Chaté et al., editors. *Mixing: chaos and turbulence*. New York: Kluwer Academic; 1999.
- [6] Cherepanov GP, Balankin AS, Ivanova VS. Fractal fracture mechanics—a review. *Engng Fract Mech* 1995;51(6):997–1033.
- [7] Creager M, Paris PC. Elastic field equations for blunt cracks with reference to stress corrosion cracking. *Int J Fract* 1967;3:247–52.
- [8] Cui Z-Y, Zhang Z-Z, Zheng S-T, Jin B-S, Xiong J-M. The analysis of stress–strain field in a finite plate with a blunt crack. *Engng Fract Mech* 1984;19:465–80.
- [9] Dimotakis PE, Catrakis HJ. Turbulence, fractals, and mixing. In: Chaté et al., editors. *Mixing: chaos and turbulence*. New York: Kluwer Academic; 1999.
- [10] Francis PH, Ko WL. The effect of root radius on the direction of crack extension under combined mode loading. *Int J Fract* 1976;12:243–52.
- [11] Goldshtein RV, Mosolov AA. Cracks with a fractal surface. *Soviet Phys Doklady* 1991;38(8):603–5.
- [12] Goldshtein RV, Mosolov AA. Fractal cracks. *J App Math Mech* 1991;56(4):563–71.
- [13] Griffith AA. The phenomenon of rupture and flow in solids. *Philos Trans R Soc London A* 1921;221:163–98.
- [14] Irwin GR. Fracture I. In: Flügge, editor. *Handbuck der Physik VI*. Springer; 1958. p. 558–90.
- [15] Kuang Z-B. The stress field near the blunt crack tip and the fracture criterion. *Engng Fract Mech* 1982;16:19–33.
- [16] McClintock FA, Irwin GR. Plasticity aspects of fracture mechanics. *ASTM STP* 1965;381:84–113.
- [17] Mosolov AA. Cracks with fractal surfaces. *Dokl Akad Nauk SSSR* 1991;319(4):840–4.
- [18] Neuber H. *Theory of notch stresses*. Berlin: Springer-Verlag; 1958.
- [19] Pugno N, Ruoff RS. Quantized fracture mechanics. *Philos Mag* 2004;84(27):2829–45.
- [20] Taylor D, Cornetti P, Pugno N. The fracture mechanics of finite crack extension. *Engng Fract Mech* 2005;72:1021–38.
- [21] Tricot C. *Curves and fractal dimension*. New York: Springer-Verlag; 1995.
- [22] Wnuk MP, Yavari A. On estimating stress intensity factors and modulus of cohesion for fractal cracks. *Engng Fract Mech* 2003;70:1659–74.
- [23] Xie H. The fractal effect of irregularity of crack branching on the fracture toughness of brittle materials. *Int J Fract* 1989;41:267–74.
- [24] Xie H, Sanderson DJ. Fractal effects of crack propagation on dynamic stress intensity factors and crack velocities. *Int J Fract* 1995;74:29–42.
- [25] Yavari A, Hockett KG, Sarkani S. The fourth mode of fracture in fractal fracture mechanics. *Int J Fract* 2000;101(4):365–84.
- [26] Yavari A, Sarkani S, Moyer ET. The mechanics of self-similar and self-affine fractal cracks. *Int J Fract* 2002;114:1–27.